**CHARACTERIZING THE IMPACT OF CRATER EJECTA ON THE SURFACE EVOLUTION OF TESSERAE.** J. L. Whitten[1] and B. A. Campbell[2], [1]Dept. Earth and Environmental Sciences, Tulane University, New Orleans, LA 70118. (jwhitten1@tulane.edu), [2]Center for Earth and Planetary Studies, Smithsonian Institution, Washington DC 20560.

**Introduction:** Tesserae represent some of the most ancient materials on Venus and, as such, preserve the longest record of surface evolution on the planet. This is particularly exciting if the past climate at the time of their formation was substantially different [1, 2] and that record was preserved by these ancient rocks. To begin to unravel the geologic record contained in tesserae, first we must understand the diversity of tesserae materials on Venus.

To get at this question, researchers have used Magellan synthetic aperture radar (SAR), topography and emissivity datasets to characterize tesserae, identified as radar-bright materials with at least two intersecting sets of tectonic structures. Geologic maps of the tesserae at various resolutions map all these materials as a single unit [e.g., 3, 4]. Recent work has sought to further classify tesserae based on changes in emissivity with topography [5], while Albach and Whitten [6] used Magellan SAR data to produce a global map of tesserae morphologies. We have also used backscatter coefficient values to subdivide tesserae [7]. These recent studies yield little substantial overlap among their defined units.

While many geologic processes have operated within tesserae since their formation (e.g., volcanism in the form of intratessera plains), impact cratering is likely to have the most influence by area. On Venus, impact craters >11 km in diameter are expected to produce parabolic ejecta deposits [8, 9], by which ejecta can be carried 100s to 1000s of kilometers away from the impact site. Most impact craters on Venus formed in the low-lying plains, generally accepted as basaltic. Therefore, most of the ejecta deposited in tesserae blanket the original surface with basaltic material. These "contaminated" areas likely contribute significantly to the diversity of currently visible tesserae surfaces on Venus.

Here, we analyze a globally distributed dataset of backscatter coefficient values from 22 different tesserae to understand how impact crater ejecta has modified their surfaces, and draw conclusions about the diversity of Venusian tesserae surface properties.

**Methodology:** We use a backscatter coefficient dataset derived from Magellan SAR left-look data (75 m/pixel). Thousands of data points were collected in 22 tesserae. Backscatter coefficient values derived from Magellan SAR data can be used to quantify surface

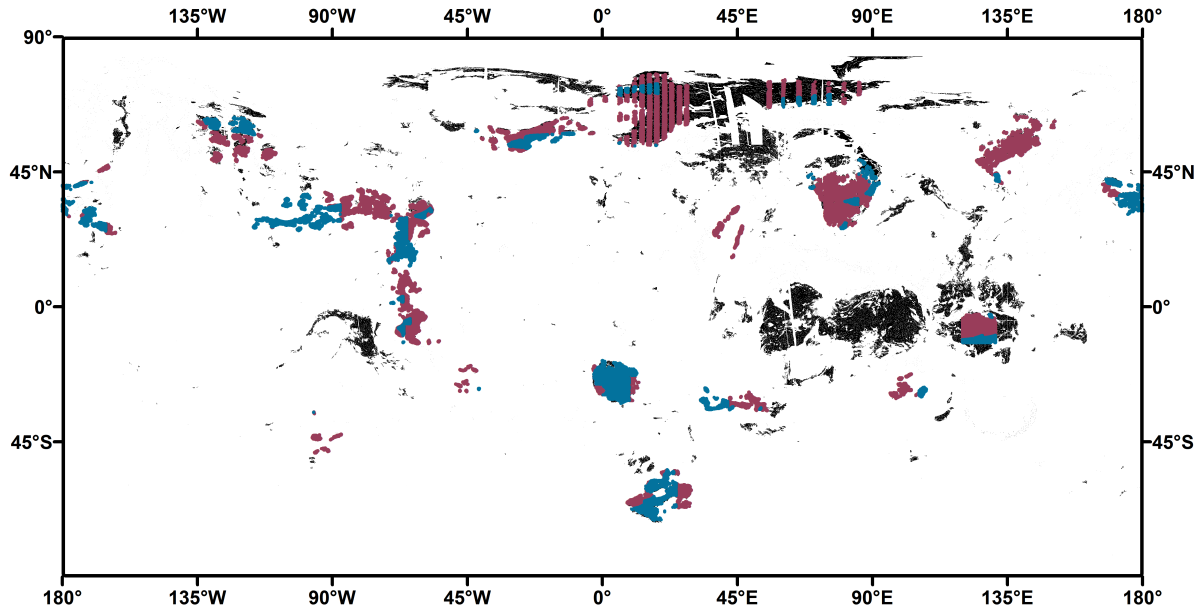


**Figure 1.** Distribution of Venusian backscatter data used in this study. Blue areas represent data that fall outside of predicted ejecta parabola margins. Maroon regions fall within the predicted margins of such extended ejecta deposits. Distal crater ejecta clearly influences the surface for a large fraction of mapped tessera terrain.

roughness [10]. Our previous work filtered these data by emissivity [7] to avoid contamination by high elevation, high dielectric materials [11]. For the research presented here, these data were further divided based on whether they fall inside or outside of predicted crater ejecta parabola margins [8, 12].

**Results and Discussion:** Approximately 70% of our backscatter dataset is within predicted parabola margins. Two of the tesserae deposits are completely "contaminated", as Mamitu and Vakko-nana tesserae are both overlapped by the predicted parabola for Mead crater (270 km in diameter). A linear trend was fit to the backscatter data versus incidence angle in each region to derive a local "scattering law". Comparing the entire backscatter dataset to the filtered data reveals that individual tessera regions "outside a parabola" better fit a trendline with angle, suggesting less variability of surface properties (Fig. 2).

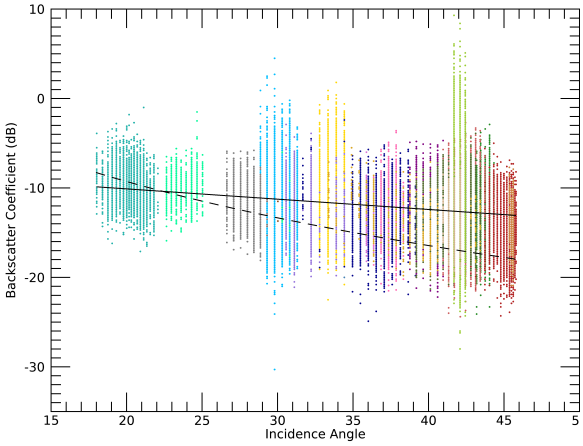


**Figure 2.** Backscatter coefficient values for data outside of crater parabolas, sorted by tesserae. There are twenty colors, each representing a different tesserae. The solid black line is our line of best fit and the dashed black line is the Muhleman scattering law applied as part of the Magellan SAR calibration effort.

We are also analyzing trends in tesserae echoes associated with craters known to have parabolic ejecta deposits: Stuart (69 km in diameter), Magnani (26 km), Boulanger (72 km), Bernhardt (25 km), Hayashi (43 km), Patti (47 km), Wazata (14 km), Mead (270 km) and Yablochkina (64 km). The expectation is that mantled-tessera backscatter coefficients decrease with smaller distances from a source crater as the deposits thicken [12].

The initial results for these 9 craters are mixed (Fig. 3). Wazata, Patti and Bernhardt have the largest change with distance, while Hayasi, Yablochkina, Mead and Boulanger show smaller ranges in backscatter coefficient values with distance. It is likely that the surface situation is more complex than a simple relationship to distance, and includes variable ejecta age, initial thickness, and orientation of potential "trapping" topography with respect to wind patterns. An analysis of the backscatter properties of parabolic ejecta superposed on low-lying plains and how it changes with

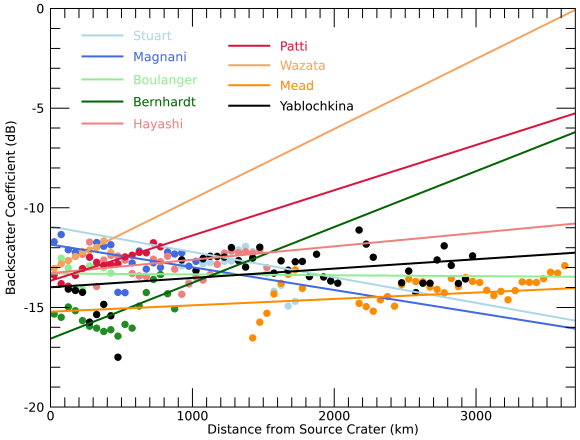


**Figure 3.** Backscatter coefficient trends associated with crater parabolic ejecta deposits that overlap with tesserae. Dots are the average backscatter measurements in 50 km distance bins and colored lines are the associated best fit linear trends.

distance will be carried out to better understand the expected patterns of backscatter in the tesserae.

**Preliminary Conclusions:** Current results indicate that upcoming missions will have to consider the presence of crater ejecta and other transported sediments when evaluating the rock types and diversity of tesserae. The work presented here explores the degree to which more narrow tesserae surface classification can be derived from analysis of backscatter values and predicted parabolic ejecta extent.

**Acknowledgments:** The backscatter data presented here were derived from Magellan data stored on the Geosciences node of the PDS. We thank M. Gilmore for sharing her GIS shapefile of predicted crater parabolas.

**References:** [1] Way M. J. et al (2016) *GRL, 43,* 8376–8383. [2] Way M. J. and Del Genio A. D. (2020) *JGR 125,* e2019JE006276. [3] Ivanov M. A. and Head J. W. (2011) *PSS, 59,* 1559–600. [4] Lang N. P. & Hansen V. L. (2010) USGS SI Map 3089. [5] Brossier, J. & Gilmore, M.S. (2021) *Icarus* 355, 114161. [6] Albach, R. S. & Whitten, J. L. (2023) *JGR*, submitted. [7] Whitten J. L. and Campbell B. A. (2023) *Geology*, submitted. [8] Campbell D. A. et al (1992) *JGR, 97,* 16249–16277. [9] Basilevsky A. T. et al (2004) *JGR, 109,* E12003. [10] Campbell B. A. (1995) USGS Open File Report 95-519. [11] Klose K. B. et al. (1992) *JGR, 97,* 16353–16369. [12] Schaller C. J. and Melosh H. J. (1998) *Icarus, 131,* 123–137.